

LLM-Enhanced Causal Discovery in Temporal Domain from Interventional Data

Peiwen Li

Tsinghua-Berkeley Shenzhen Institute
Tsinghua University, Shenzhen, China
Alibaba Cloud, Hangzhou, China
lpw22@mails.tsinghua.edu.cn

Xin Wang*

Department of Computer Science and
Technology, BNRist
Tsinghua University, Beijing, China
xin_wang@tsinghua.edu.cn

Zeyang Zhang

Department of Computer Science and
Technology
Tsinghua University, Beijing, China
zy-zhang20@mails.tsinghua.edu.cn

Yuan Meng*

Department of Computer Science and
Technology
Tsinghua University, Beijing, China
yuanmeng@mail.tsinghua.edu.cn

Fang Shen

Alibaba Cloud
Hangzhou, China
ziru.sf@alibaba-inc.com

Yue Li

Alibaba Cloud
Hangzhou, China
yueqian.ly@alibaba-inc.com

Jialong Wang*

Alibaba Cloud
Hangzhou, China
quming.wjl@alibaba-inc.com

Yang Li

Tsinghua-Berkeley Shenzhen Institute
Tsinghua University
Shenzhen, China
yangli@sz.tsinghua.edu.cn

Wenwu Zhu*

Department of Computer Science and
Technology, BNRist
Tsinghua University, Beijing, China
wwzhu@tsinghua.edu.cn

ABSTRACT

In the field of Artificial Intelligence for Information Technology Operations (AIOps), causal discovery is pivotal for operation and maintenance of graph construction, facilitating downstream industrial tasks such as root cause analysis. Temporal causal discovery, as an emerging method, aims to identify temporal causal relationships between variables directly from observations by utilizing interventional data. However, existing methods mainly focus on synthetic datasets with heavy reliance on interventional targets and ignore the textual information hidden in real-world systems, failing to conduct causal discovery for real industrial scenarios. To tackle this problem, in this paper we propose to investigate temporal causal discovery in industrial scenarios, which faces two critical challenges: 1) how to discover causal relationships without the interventional targets that are costly to obtain in practice, and 2) how to discover causal relations via leveraging the textual information in systems which can be complex yet abundant in industrial contexts. To address these challenges, we propose the **RealTCD** framework, which is able to leverage domain knowledge to discover temporal causal relationships without interventional targets. Specifically, we first develop a score-based temporal causal discovery method capable of discovering causal relations for root cause analysis without relying on interventional targets through

strategic masking and regularization. Furthermore, by employing Large Language Models (LLMs) to handle texts and integrate domain knowledge, we introduce LLM-guided meta-initialization to extract the meta-knowledge from textual information hidden in systems to boost the quality of discovery. We conduct extensive experiments on both simulation and real-world datasets to show the superiority of our proposed **RealTCD** framework over existing baselines in discovering temporal causal structures.

CCS CONCEPTS

• **Computing methodologies** → *Causal reasoning and diagnostics; Temporal reasoning.*

KEYWORDS

Large Language Model, Causal Discovery, Time series, Intervention

ACM Reference Format:

Peiwen Li, Xin Wang, Zeyang Zhang, Yuan Meng, Fang Shen, Yue Li, Jialong Wang, Yang Li, and Wenwu Zhu. 2024. LLM-Enhanced Causal Discovery in Temporal Domain from Interventional Data. In *Proceedings of ACM Conference (Conference'17)*. ACM, New York, NY, USA, 13 pages. <https://doi.org/10.1145/nnnnnnn.nnnnnnn>

1 INTRODUCTION

The advent of Artificial Intelligence for Information Technology Operations (AIOps) has revolutionized the way we manage and operate complex information systems. Causal discovery plays a pivotal role in understanding the intricate network of dependencies and influences within these systems [2, 27, 52, 54], offering invaluable insights for various downstream industrial tasks in AIOps, including anomaly detection [49] and root cause analysis [42, 48] etc. For instance, by equipping AIOps with the ability to accurately identify the underlying causal structures, AIOps systems can effectively detect abnormal behaviors and determine the underlying

*Corresponding authors

Permission to make digital or hard copies of all or part of this work for personal or classroom use is granted without fee provided that copies are not made or distributed for profit or commercial advantage and that copies bear this notice and the full citation on the first page. Copyrights for components of this work owned by others than the author(s) must be honored. Abstracting with credit is permitted. To copy otherwise, or republish, to post on servers or to redistribute to lists, requires prior specific permission and/or a fee. Request permissions from permissions@acm.org.
Conference'17, July 2017, Washington, DC, USA

© 2024 Copyright held by the owner/author(s). Publication rights licensed to ACM.
ACM ISBN 978-x-xxxx-xxxx-x/YY/MM
<https://doi.org/10.1145/nnnnnnn.nnnnnnn>

causes of system failures, thus leading to enhanced operational efficiency and improved decision-making processes in industry.

Temporal causal discovery, as an emerging approach, aims to directly identify temporal causal relationships between variables based on observational data, with the utilization of interventional data. This group of methods have gained significant attention in recent years due to their promising potential to uncover causal dependencies in dynamic systems. For example, Brouillard et al. [6] and Li et al. [23] employ temporal causal discovery methods to leverage various types of interventional data and have achieved remarkable progress in discovering the underlying temporal causal relationships.

However, the existing studies mainly focus on studying synthetic datasets, which strongly rely on interventional targets and ignore the intricate complexities and nuances hidden in real-world systems, failing to conduct causal discovery for real industrial scenarios. In this paper, we tackle this problem by studying temporal causal discovery in industrial scenarios, which is non-trivial and poses the following two critical challenges:

- How to discover casual relationships without the interventional targets that are normally costly to obtain in practice?
- How to discover causal relations via leveraging the textual information in systems which can be complex yet abundant in industrial contexts?

To address these challenges, we propose the **RealTCD** framework, which is able to leverage the textual information from real-world systems to discover temporal causal relationships without interventional targets. Specifically, we first develop a score-based temporal causal discovery method that learns the underlying causal relationship without interventional targets through strategic masking and regularization. We impose regularizations on both the adjacency matrix and interventional family within the context of the regularized maximum log-likelihood score, as well as and optimize them in a joint manner. In this way, the costly interventional targets are not required for boarder applications in real-world industrial scenarios. Subsequently, by leveraging Large Language Models (LLMs) to handle texts, we introduce LLM-guided meta-initialization that infers and initializes the inherent causal structures from the textual information in systems for the aforementioned discovery process, which incorporates the domain knowledge while upholding the theoretical integrity of temporal causal discovery. Extensive experiments on both simulation and real-world datasets demonstrate the superiority of our **RealTCD** framework over existing baselines in terms of discovering temporal causal structures. The deeper analyses also show that our method can effectively discover the underlying temporal causal relationship without interventional targets in industrial scenarios. In summary, our main contributions are as follows:

- We study the problem of temporal causal discovery in industrial scenarios. To the best of our knowledge, we are the first to solve the problem with Large Language Models (LLMs) and without interventional targets.
- We propose the **RealTCD** framework, including two specially designed modules, i.e., score-based temporal causal discovery and LLM-guided meta-initialization, which is able to leverage the textual information in systems to discover temporal causal

relationships without interventional targets in industrial scenarios.

- Extensive experiments on both simulation and real-world datasets demonstrate the superiority of our framework over several baselines in discovering temporal causal structures without interventional targets.

2 RELATED WORK

2.1 Causal Discovery in Temporal Domain

Existing theoretical evidence confirms the fact that when interventional data is readily available, it greatly amplifies the process of identifying underlying causal structures [11, 12, 38, 55]. However, the expansion of research in this particular domain has been rather restricted due to substantial obstacles rooted in designing intervention experiments as well as gathering the requisite data. Jaber et al. [16] took up the challenge of learning causal graphs entailing latent variables, derived from a combination of observational and interventional distributions where the interventional aims are yet to be known. To address this concern, the study proposed an approach utilizing a Ψ -Markov property. Addanki et al. [1] put forth a randomized algorithm, characterized by p -colliders, that recovers the comprehensive causal graph, whilst also minimizing the intervention expense. Further, an adaptable method for causality detection, Brouillard et al. [6], notably benefits from different categories of interventional data and incorporates refined neural architectures like the normalizing flows, operating under continuous constraints. Li et al. [23] attempt to discover the temporal cause from observation data, while the intervention labels, which are hard to obtain in real-world scenarios, are indispensable for the proposed algorithm, limiting its application in practice. In comparison, in this paper, we focus on the setting of discovering the temporal causal relationship without intervention labels.

2.2 LLM for Causal Discovery

Recently, there have been several works about utilizing large language models (LLMs) for causal discovery [3, 5, 10, 15, 18, 21, 24, 36, 40, 46] and dynamic graph [43, 44, 50, 53]. Ban et al. [4] explore the use of LLMs as advanced causal architects to discover causal relationships from data and highlight the potential of LLMs in transforming traditional query tools into powerful tools for causal inference. Chan et al. [8] focus on evaluating the performance of ChatGPT in capturing sentence-level temporal, causal, and discourse relations. Chen et al. [9] explore how incorporating LLMs can enhance causal discovery methods by reducing biases and improving the accuracy of learned causal structures and propose to mitigate prior errors in causal structure learning by leveraging LLM-driven prior knowledge. Kiciman et al. [22] explore the role of LLMs in advancing causal discovery, counterfactual reasoning, and actual causality tasks, and highlight the potential of large language models in opening new frontiers for causal reasoning. Long et al. [25] investigate the question of whether large language models can build causal graphs, and explore whether GPT-3 in understanding the causal relationships between variables in the medical context. To the best of our knowledge, we are the first to utilize LLMs in the field of temporal causal discovery.

3 PRELIMINARY

3.1 Dynamic Causal Graphical Model

Since causal graphical models (CGMs) support interventions compared with standard Bayesian Networks, we introduce the dynamic causal graphical models (DyCGMs) extended from CGMs in order to formulate interventions between variables across time slices. Suppose that there are d different measuring points in a system, and we consider causality within p time-lagged terms. Therefore, the object of our study on temporal causal discovery is actually $(p+1) \times d$ random variables $N_{0,1}, \dots, N_{0,d}, \dots, N_{p,1}, \dots, N_{p,d}$, where $N_{k,l}, k \in \{0, \dots, p\}, l \in \{1, \dots, d\}$ denotes the k time-lagged version of the l th measuring point. For the convenience of subsequent presentation, we abbreviate the above variables in order as $X_i, i \in \{1, \dots, (p+1)d\}$.

Based on this, a DyCGM is defined by the distribution P_X over the vector $X = (X_1, \dots, X_{(p+1)d})$ and a DAG $\mathcal{G} = (V, E)$. To be specific, each node $i \in V = \{1, \dots, (p+1)d\}$ is related with a random variable $X_i, i \in \{1, \dots, (p+1)d\}$, and each edge $(i, j) \in E$ represents a direct causal relation from variable X_i to X_j . Under the Markov assumption of the distribution P_Y and graph \mathcal{G} , the joint distribution can be factorized as

$$p(x_1, \dots, x_{(p+1)d}) = \prod_{j=1}^{(p+1)d} p_j(x_j | x_{\pi_j^{\mathcal{G}}}), \quad (1)$$

where $\pi_j^{\mathcal{G}}$ is the set of parents of the node j in the graph \mathcal{G} , and $x_{\pi_j^{\mathcal{G}}}$ denotes the entries of the vector x with indices in $\pi_j^{\mathcal{G}}$.

We also assume *causal sufficiency*, which means there is no hidden common cause that is causing more than one variable in X [32].

3.2 Intervention

An intervention on a variable x_j corresponds to replacing its conditional density $p_j(x_j | x_{\pi_j^{\mathcal{G}}})$ by a new one. Apart from that, we define the *interventional target*, a set $I \subseteq V$ consisting of the variables being intervened simultaneously, and the *interventional family* $\mathcal{I} := (I_1, \dots, I_Q)$, where Q is the number of interventions. To be specific, the observational setting, where no variables were intervened, is always known and denoted by $I_1 := \emptyset$. The q th interventional joint density can be represented as

$$p^{(q)}(x_1, \dots, x_{(p+1)d}) := \prod_{j \notin I_q} p_j^{(1)}(x_j | x_{\pi_j^{\mathcal{G}}}) \prod_{j \in I_q} p_j^{(q)}(x_j | x_{\pi_j^{\mathcal{G}}}). \quad (2)$$

Note that, in the temporal domain, merely the contemporary variables $N_{0,1}, \dots, N_{0,d}$, i.e. X_1, \dots, X_d can be intervened and be in an interventional target, as only time-lagged variables $N_{k,l}, k \in \{1, \dots, p\}, l \in \{1, \dots, d\}$, i.e. $X_i, i \in \{d+1, \dots, (p+1)d\}$ and other contemporary variables $N_{0,l}, l \in \{1, \dots, d\} \setminus \{j\}$, i.e. $X_i, i \in \{0, \dots, d\} \setminus \{j\}$ can affect a particular contemporary variable $N_{0,j}$, i.e. X_j .

Meanwhile, there are two types of interventions: 1) imperfect (or soft, parametric) interventions is the general type depicted below, and 2) perfect interventions (or hard, structural) [16] is a special case that removes the dependencies of an intervened node $j \in I_q$ on its parent nodes, i.e. $p_j^{(q)}(x_j | x_{\pi_j^{\mathcal{G}}}) = p_j^{(q)}(x_j)$ in equation (2).

4 METHOD

In order to make the causal discovery process able to be applied to the real industrial scene effectively, we propose the **RealTCD** framework as shown in Figure 1, including two modules: 1) in the module **Score-based Temporal Causal Discovery**, data from normal state and abnormal state of a system under AIOps are modeled as observational data and interventional data respectively, and relaxation is done to the condition that the label of interventional targets is known, making the algorithm easier to apply to real scenes; 2) in the module **LLM-guided Meta Initialization**, LLM is leveraged to introduce the domain knowledge and system structure information in text types and to preliminarily obtain possible causal relations from them as initialization for the discovery process.

4.1 Score-based Temporal Causal Discovery

In this section, we introduce a score-based purely data-driven temporal causal discovery from interventional data with unknown interventional targets.

4.1.1 Raw data. The raw data we used in our method as shown in Figure 1 refers to a set of input temporal data that includes both observational and interventional data. Observational data refers to standard data without any interventions or anomalies, while interventional data contains interventions as discussed in Section 3.2, or represents abnormal data in real-world datasets. The colored columns in interventional data represent the time series of intervened (or anomalous) variables. This data encompasses d different measurement points in a system over p time-lagged terms, as described in Section 3.1. Additionally, there may be multiple sets of interventional data, each corresponding to different interventional targets or anomalies.

4.1.2 Model conditional densities. To begin with, we use neural networks to model conditional densities. Firstly, we encode the DAG \mathcal{G} with a binary adjacency matrix $M^{\mathcal{G}} \in \{0, 1\}^{(p+1)d \times (p+1)d}$ which acts as a mask on the neural network inputs. Similarly, we encode the interventional family \mathcal{I} with a binary matrix $R^{\mathcal{I}} \in \{0, 1\}^{Q \times (p+1)d}$, where $R_{qj}^{\mathcal{I}} = 1$ means that X_j is an intervened node in the interventional target set I_q . Then, following equation (2), we further model the joint density of the q th intervention by

$$f^{(q)}(x; M^{\mathcal{G}}, R^{\mathcal{I}}, \phi) := \prod_{j=1}^{(p+1)d} \tilde{f}(x_j; \text{NN}(M_j^{\mathcal{G}} \odot x; \phi_j^{(1)}))^{1-R_{qj}^{\mathcal{I}}} \tilde{f}(x_j; \text{NN}(M_j^{\mathcal{G}} \odot x; \phi_j^{(q)}))^{R_{qj}^{\mathcal{I}}}, \quad (3)$$

where $\phi := \{\phi^{(1)}, \dots, \phi^{(Q)}\}$, the NN's are neural networks parameterized by $\phi_j^{(1)}$ or $\phi_j^{(q)}$, the operator \odot denotes the Hadamard product (element-wise) and $M_j^{\mathcal{G}}$ denotes the j th column of $M^{\mathcal{G}}$, enabling $M_j^{\mathcal{G}} \odot x$ to select the parents of node j in the graph \mathcal{G} .

4.1.3 Score for unknown interventional targets. Based on the NN conditional densities in equation (3), we can firstly formulate the following **regularized maximum log-likelihood score** as the

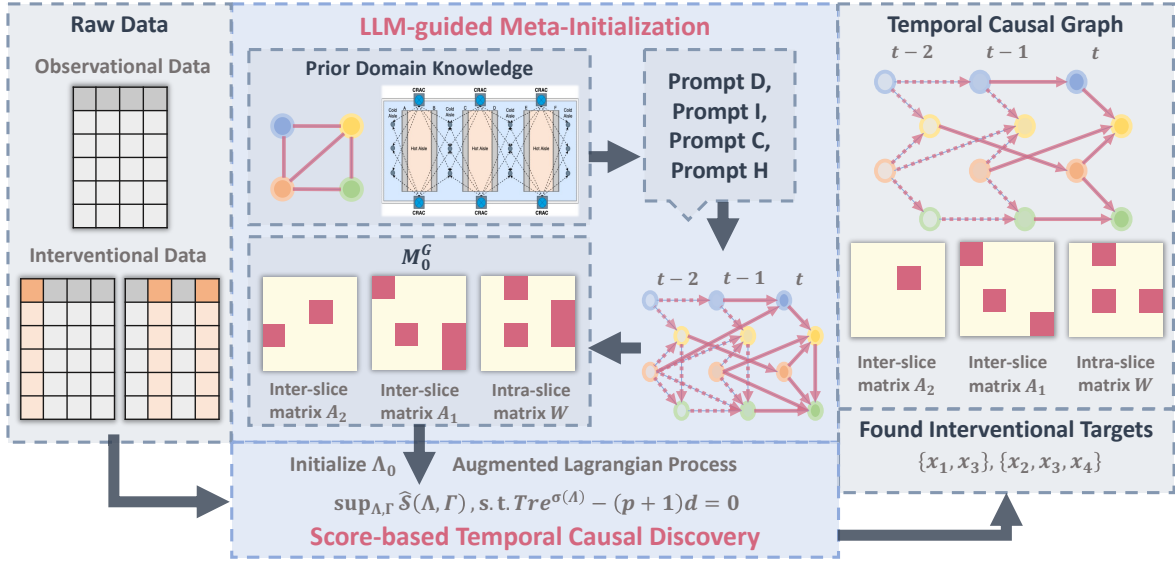


Figure 1: The framework of our proposed method RealTCD. Given the system textual information and temporal data without interventional targets, the LLM-guided Meta-Initialization module leverages LLMs to extract the domain knowledge and obtain the potential causal relations as the initialization adjacency matrix $M_0^{\mathcal{G}}$. Then, the Score-based Temporal Causal Discovery module utilizes an augmented Lagrangian process to optimize the score for unknown interventional targets under constraints, where the Λ_0 is initialized with $M_0^{\mathcal{G}}$. In this way, the proposed RealTCD leverages the system textual information to discover temporal causal relationships without interventional targets.

basic score for known interventional targets' setting:

$$\mathcal{S}_{\mathcal{I}^*}(\mathcal{G}) := \sup_{\phi} \sum_{q=1}^Q \mathbb{E}_{X \sim p^{(q)}} \log f^{(q)}(X, M^{\mathcal{G}}, R^{\mathcal{I}^*}, \phi) - \lambda |\mathcal{G}|, \quad (4)$$

where the ground truth interventional family (containing the interventional targets) $\mathcal{I}^* := (\mathcal{I}_1^*, \dots, \mathcal{I}_Q^*)$ is known and $p^{(q)}$ stands for the q th ground truth interventional distribution, $|\mathcal{G}|$ represents the number of edges in the causal graph. By maximizing the score in equation (4), we can get an estimated DAG $\hat{\mathcal{G}}$ that is \mathcal{I}^* -Markov equivalent to the true DAG \mathcal{G}^* [6], under the condition that the ground truth interventional family is known.

After that, we assume that the interventional targets are unknown. To still be able to utilize the special information from interventional data, we propose to jointly optimize the adjacency matrix and interventional family as well as the NN's parameters, thus, reaching the two optimization goals simultaneously. To be specific, a regularization term for the interventional family is added to the above score, and we form the score for unknown interventional targets:

$$\mathcal{S}(\mathcal{G}, \mathcal{I}) := \sup_{\phi} \sum_{q=1}^Q \mathbb{E}_{X \sim p^{(q)}} \log f^{(q)}(X, M^{\mathcal{G}}, R^{\mathcal{I}}, \phi) - \lambda |\mathcal{G}| - \lambda_R |\mathcal{I}|, \quad (5)$$

where $|\mathcal{I}| = \sum_{q=1}^Q |\mathcal{I}_q|$ counts the total number of intervened nodes in data.

The following theorem guarantees the identification of the temporal causal graph as well as the interventional family under the setting that interventional targets are unknown, which can be proved similarly as in our previous work [23].

THEOREM 4.1 (UNKNOWN TARGETS TEMPORAL CAUSAL DAG IDENTIFICATION). *Suppose \mathcal{I}^* is such that $\mathcal{I}_1^* := \emptyset$. Let \mathcal{G}^* be the ground truth temporal DAG and $(\hat{\mathcal{G}}, \hat{\mathcal{I}}) \in \operatorname{argmax}_{\mathcal{G} \in \text{DAG}, \mathcal{I}} \mathcal{S}(\mathcal{G}, \mathcal{I})$. Under the assumptions that: 1) the density model has enough capacity to represent the ground truth distributions; 2) \mathcal{I}^* -faithfulness holds; 3) the density model is strictly positive; 4) the ground truth densities $p^{(q)}$ have finite differential entropy. For $\lambda, \lambda_R > 0$ small enough, $\hat{\mathcal{G}}$ is \mathcal{I}^* -Markov equivalent to \mathcal{G}^* and $\hat{\mathcal{I}} = \mathcal{I}^*$.*

4.1.4 Maximize the score. Subsequently, to allow the gradient-based stochastic optimization process, we relax the above score by taking $M^{\mathcal{G}}$ and $R^{\mathcal{I}}$ as a random matrix respectively, where $M_{ij}^{\mathcal{G}} \sim B(1, \sigma(\alpha_{ij}))$ and $R_{qj}^{\mathcal{I}} \sim B(1, \sigma(\beta_{qj}))$, B represents the Bernoulli distribution, σ is the sigmoid function and α_{ij}, β_{qj} are scalar parameters. We group these α_{ij} s into a matrix $\Lambda \in \mathbb{R}^{(p+1)d \times (p+1)d}$, and β_{qj} s into a matrix $\Gamma \in \mathbb{R}^{Q \times (p+1)d}$. After that, we rely on *augmented Lagrangian procedure* [56] to maximize the following score:

$$\hat{\mathcal{S}}(\Lambda, \Gamma) := \sup_{\phi} \mathbb{E}_{M \sim \sigma(\Lambda)} \left[\mathbb{E}_{R \sim \sigma(\Gamma)} \left[\sum_{q=1}^Q \mathbb{E}_{X \sim p^{(q)}} \log f^{(q)}(X; M, R^{\mathcal{I}^*}, \phi) - \lambda \|M\|_0 - \lambda_R \|R\|_0 \right] \right], \quad (6)$$

under the acyclicity constraint:

$$\sup_{\Lambda, \Gamma} \hat{\mathcal{S}}(\Lambda, \Gamma), \text{ s.t. } \text{Tr } e^{\sigma(\Lambda)} - (p+1)d = 0. \quad (7)$$

Moreover, as for the gradient of the score w.r.t. α_{ij} and β_{qj} , following the general dealing method in continuous optimization for causal discovery [19, 29], we estimate Λ and Γ by *Straight-Through Gumbel estimator*, which means that Bernoulli samples are used in the forward pass and Gumbel-Softmax samples are used in the backward pass.

Overall, the learnable parameters in the process are ϕ, Λ, Γ , and the estimated adjacency matrix reflecting temporal causal relations is $\sigma(\Lambda)$ and the estimated potential interventional family is $\sigma(\Gamma)$.

Since we only focus on influences on X_1, \dots, X_d from other variables, we set $\Lambda[:, d+1 : (p+1)d]$, i.e. the meaningless part $M^{\mathcal{G}}[:, d+1 : (p+1)d]$, to zero before training.

4.2 LLM-guided Meta Initialization

In this section, we introduce the detailed method of using LLM to bring in domain knowledge and extra prior information [7, 31] so that the potential temporal causal relations are obtained to guide the data-driven optimization process.

Prompts of LLMs. We describe the system into prompts as queries to the LLMs for possible temporal causal relationships. One prompt example is shown in Table 1, where the underlined units are indispensable and the others are optional. We also provide the more detailed example of the prompt used for the real-world dataset in our experiments in Appendix B.

We have implemented strategies to mitigate such biases, notably through the use of tailored prompts (Prompt D and Prompt I). Prompt D is designed to clarify the causal discovery tasks for the LLMs and align them with the domain knowledge inherent to the LLMs themselves. Prompt I further introduces data and domain knowledge consistent with the subsequent causal discovery tasks to the LLMs, such as context descriptions, physical structures, and generating rules, to ensure that the meta-initialization process is as unbiased as possible.

Through the list of tuples LLM offered to us, we then construct the adjacency matrix $M_0^{\mathcal{G}}$ to denote the causal structure learned from LLM. Note that, these results may not be the certainly correct causality conform to a causal definition, but a range of potential causality based on the domain information. We further design two modules to incorporate the meta-initialization information.

Guide temporal causal discovery from data. By initiating $M^{\mathcal{G}}$ or to say Λ of the module score-based temporal causal discovery as the results $M_0^{\mathcal{G}}$ from the module LLM-guided meta initialization before training and optimization, we not only lead the direction of the data-driven optimization process but also guarantee the theoretical integrity of the temporal causal discovery from interventional data.

Extract weight. Eventually, we obtain the estimated full weight matrix $\hat{F} = \sigma(\Lambda)$ of graph \mathcal{G} . Then, we form the adjacency matrix $\hat{M}^{\mathcal{G}}$ of the graph by adding an edge whenever $\sigma(\Lambda) > 0.5$ is acyclic. Finally, we can extract the intra-slice matrix $\hat{W} = \hat{M}^{\mathcal{G}}[1 : d, 1 : d]$ and inter-slice matrix $\hat{A}_k = \hat{M}^{\mathcal{G}}[kd+1 : (k+1)d, 1 : d]$ for each time

Table 1: Example prompt for LLM-guided Meta Initialization.

Prompt Definition
Role: "You are an exceptional temporal causal discovery analyzer, with in-depth domain knowledge in ... (e.g. the intelligent operation and maintenance of data center air-conditioning systems)."
Introduction: "A directed temporal causal relationship between variables x_u and x_v can be represented as a tuple (x_u, x_v, t) , signifying that the variable x_u , lagging t time units, causally influences the current state of variable x_v . The tuple $(x_u, x_v, 0)$ denotes contemporaneous causality if $t=0$; if $t>0$, the tuple (x_u, x_v, t) indicates time-lagged causality. Note that when $t=0$, i.e. in $(x_u, x_v, 0)$, x_u and x_v must be different variables, as intra-slice self-causality is not considered. Also, $(x_u, x_v, 0)$ and (x_u, x_v, t) for $t>0$ have the possibility to coexist, suggesting that contemporaneous and time-lagged causality between two variables might simultaneously occur sometimes. Our task is to unearth all the possible temporal causal relationships among variables, grounded on the subsequent information."
Prompt Information
Domain knowledge: Depending on the application scenarios, it might be: 1) A <i>context description</i> of a specific industrial scenario or AIOps scenario. 2) The <i>physical structure</i> of the system, containing the <i>location</i> information of each entity or variable. 3) The abstract <i>generating rules</i> of time series.
Data: Providing a piece of past time series may help LLM understand the variables and their relations better.
Prompt Causal Discovery in Temporal Domain
Task: "Please identify all temporal causal relations among the n variables (x_1, \dots, x_n) , considering only contemporaneous and p time-lagged causality. Conclude your response with the full answer as a Python list of tuples (x_u, x_v, t) after 'Answer:'. Don't simplify and just give me some examples. You should cover all possible relationships in your answer."
Prompt Hint
Implication: We can offer a thinking path to the LLM model as a guide of how we want it to utilize the prior information we gave to it or its own knowledge and deduct the answer.
Chain of Thought (CoT): "Proceed methodically, step by step." By simply adding a zero-shot CoT prompt, the LLM model could output its answer with its path of thought, making the process more interpretable and easy for humans to understand, check, and correct immediately [26, 45]. Furthermore, if we can provide an example that contains the correct thought path and result as input, the one-shot CoT may achieve an even better result.

lag $k = 1, \dots, p$. They reflect causal relations of these d variables in both a contemporary and time-lagged manner.

The overall framework and algorithm of **RealTCD** are summarized in Figure 1 and Algorithm 1 respectively.

5 EXPERIMENTS

5.1 Setups

5.1.1 Baselines. To evaluate the effectiveness of our method, we compare with the following models as baselines:

Algorithm 1 The overall algorithm for RealTCD**Require:** All kinds of prior knowledge

- 1: Generate prompt as described in Table 1
- 2: Obtain the causal results from LLM and transfer into matrix $M_0^{\mathcal{G}}$

Require: $M_0^{\mathcal{G}}$, hyperparameter λ , λ_R , hyperparameter for augmented Lagrangian process

- 3: Transfer the constrained problem defined by equation (6), (7) into the form of unconstrained problem following augmented Lagrangian
- 4: Initialize Λ_0 by $M_0^{\mathcal{G}}$, and also initialize ϕ_0, Γ_0 , max_iteration U , Lagrangian multiplier γ_0 and penalty coefficient μ_0
- 5: **while** $0 \leq t \leq U$ and $h(\Lambda) := \text{Tr } e^{\sigma(\Lambda)} - (p+1)d > 10^{-8}$ **do**
- 6: Solve the t th unconstrained subproblem using stochastic gradient descent algorithm (we use RMSprop)
- 7: Get the sub solution $\phi_t^*, \Lambda_t^*, \Gamma_t^*$, and initialize $\phi_{t+1}, \Lambda_{t+1}, \Gamma_{t+1}$ by them
- 8: Update γ_{t+1} and μ_{t+1}
- 9: $t = t + 1$
- 10: **end while**
- 11: Form the causal graph by adding an edge whenever $\sigma(\Lambda) > 0.5$ is acyclic

- **DYNOTEARS** [30]: As DYNOTEARS is a method focused on fitting the exact values of time series, it outputs quantitative weight values. We set threshold value of W and A to be 0.5.
- **PCMCI** [35]: We use results with a significance level of 0.01.
- **TECDI** [23]: It is a temporal causal discovery methods require both interventional data and interventional targets.
- **NeuralGC** [37]: Since NeuralGC only learns contemporaneous relationships, we use W_{full} defined as below to compress both contemporaneous and time-lagged causal relationships learnt from RealTCD into a single metric for comparison with NeuralGC, which does not differentiate between these 2 types.

$$W_{\text{full}}(i, j) = \begin{cases} 1, & W(i, j) + \sum_{k=1}^p A_k(i, j) > 0 \\ 0, & \text{otherwise} \end{cases} \quad (8)$$

This formulation captures the entire causal relationship from i to j , assuming a relationship exists if any contemporaneous or time-lagged relationship is present.

The distinction in method selection across different settings was intentional and aligned with the capabilities of each algorithm: Since PCMCI and DYNOTEARS are designed for causal structure learning from observational data and can not incorporate interventional data, we included them in the "Unknown" interventional targets setting. As for TECDI, we use the same data with RealTCD, i.e. both observational and interventional data (or abnormal data in real datasets), to run it, since it can utilize the interventional data. However, for other baseline models that are unable to bring in interventional data, we have ensured a fair comparison to some extent by keeping the overall sample size consistent across all models, while using only observational data (or normal data in real datasets) for the baseline models.

5.1.2 Synthetic datasets. We generate temporal data in two steps:

- Sample intra DAG and inter DAG following the *Erdős-Rényi* scheme, then sample parameters in weighted adjacency matrix, where elements in intra-slice matrix W are uniformly from $[-1.0, -0.25] \cup [0.25, 1.0]$ and elements in inter-slice matrixes A_k are uniformly from $[-1.0\alpha, -0.25\alpha] \cup [0.25\alpha, 1.0\alpha]$, $\alpha = 1/\eta^k$, $\eta \geq 1$, $k = 1, \dots, p$.
- Generate time series consistent with the sampled weighted graph following the standard structural vector autoregressive (SVAR) model[34]: $Y_0 = Y_0W + Y_1A_1 + \dots + Y_pA_p + Z$, where Z is random variables under the normal distribution. Then, sample interventional targets from nodes in Y_0 , and generate perfect interventional data by cutting off the dependency of intervened nodes on their parents, i.e. setting W_{ij} and A_{kij} to zero, where x_j is the variable in interventional targets and $x_i \in x_{\pi_j^{\mathcal{G}}}$.

Before training, all data are normalized by subtracting the mean and dividing by the standard deviation. We experimented on two simulated datasets: Dataset 1 contains 5 nodes, their 1 time-lagged variables and 5 different interventional targets, each of which covers a single different node. Dataset 2 contains 10 nodes, their 1 time-lagged variables and 10 different interventional targets, each of which covers a single different node. We initially chose to limit our datasets to a time delay of 1 to facilitate the evaluation and presentation. However, it is indeed feasible to increase the time delay of the data.

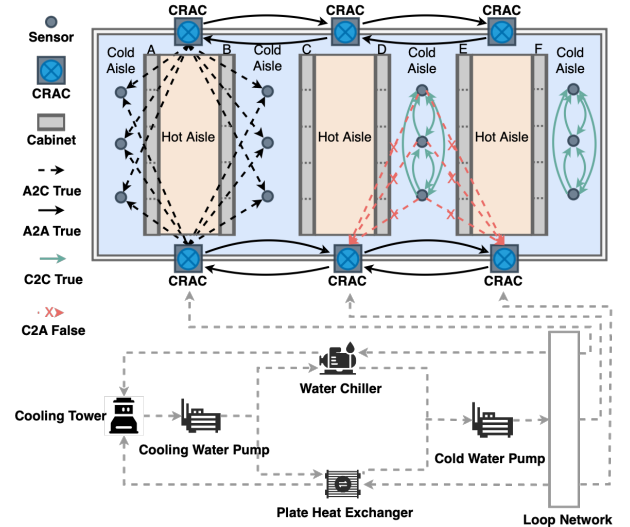


Figure 2: A typical data center cooling system diagram.

5.1.3 Real-world data center datasets. In contemporary data centers, the stability of IT equipment operation is paramount. To this end, sophisticated air conditioning systems are employed to manage the heat generated by the equipment, thereby sustaining a consistent indoor temperature. As illustrated in Figure 2, a standard data center room is methodically organized with rows of equipment (labeled A, B, C, D, and so forth). These rows are strategically separated by physical barriers, effectively isolating adjacent cabinet rows to impede the intermingling of hot and cold air streams.

Computer Room Air Conditioners (CRACs), strategically positioned on both sides of the room, facilitate a closed-loop configuration, essential for preserving a stable environmental condition. The deployment of multiple sensors within the cold aisle is a critical aspect of this setup, providing real-time temperature data. This continuous monitoring is crucial for ensuring the uninterrupted delivery of cold air, thereby allowing for prompt adjustments that are essential for the consistent operation of IT equipment.

Data acquisition. The data used in this study was obtained from a specific data center at Alibaba. It covers monitoring data from a cooling system of a particular room from January 1st, 2023 to May 1st, 2023, and includes 38 variables in total. These variables comprise 18 cold aisle temperatures from sensors and 20 air conditioning supply temperatures from CRACs. We collected several time series of these 38 variables during normal as well as abnormal states. For the latter, data was sampled within 20 minutes of the occurrence of the abnormality, with each sampling interval being 10 seconds. Anomaly points were identified by learning the normal distribution range from historical data, using the n - σ method. Any data points that fall outside of the n - σ range (e.g., 3 to 5) of it selves are extracted as anomaly time points.

A more detailed description of synthetic and real-world datasets generation is in Appendix A.

5.1.4 Evaluation metrics.

For synthetic datasets. We leverage the following two main metrics to evaluate the performance of the proposed method on learning causal graph: i) the structural Hamming distance (**SHD**), which calculates the number of different edges (either reversed, missing or redundant) between two DAGs; ii) the structural interventional distance (**SID**), which represents the difference between two DAGs according to their causal inference conditions [33].

For real-world datasets. Given the absence of ground truth DAGs in real case, we employ 4 types of performance metrics based on prior knowledge to assess the algorithms' efficacy in learning causal graphs. These metrics mainly consider the physical location relationships within the room, shown in figure 2. Specifically: i) **A2C True** counts the correctly identified causal edges from air conditioning supply temperatures (A) to the temperatures of adjacent cold aisles (C), assuming that A influences C. ii) **A2A True** counts the correctly identified causal edges between adjacent air conditioning units, assuming mutual influences among them. iii) **C2C True** counts the correctly identified causal edges between temperatures in the same column of cold aisles, assuming direct interactions among them. iv) **C2A False** counts the incorrectly identified causal edges from cold aisle temperatures (C) to air conditioning supply temperatures (A), as such causality is implausible given that downstream variables (C) cannot influence upstream variables (A).

5.2 Main Results

5.2.1 On synthetic datasets. The results on synthetic datasets are reported in Table 2. We can find that on both datasets, our method achieves significantly better results than baseline models on both metrics SHD and SID of the overall structures. The standard deviation of each metric is relatively small as well. Especially for the

dataset with 10 nodes, our improvement over other baselines is more obvious, indicating that our method indeed has more advantages when dealing with a **large number of variables**, making the optimization more **focused** and **effective**. RealTCD consistently achieves better performance in each setting. Specifically, the "Known" targets setting performs better than the "Unknown" targets setting, which is reasonable since the former employs ground-truth interventional target labels for training. However, it is always impossible to obtain ground-truth interventional targets in real-world applications, making the proposed RealTCD for the setting of interventional data with unknown targets highly practical.

Figure 3 and Figure 4 show example results of the temporal causal DAG and interventional targets simultaneously obtained through RealTCD. In Figure 4, each row represents a contemporary node, while each column in the matrix is a regime corresponding to an interventional family, where the first column represents the observational data, and the following 5 columns represent 5 different interventional data respectively. The pink cells are the learned/ground truth interventional targets in each regime. It shows that our method is able to find the correct temporal causal graph and interventional targets at the same time.

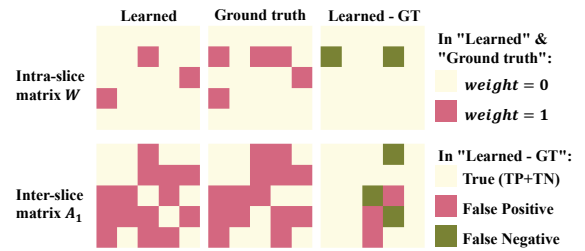


Figure 3: A showcase of the DAG results on synthetic data.

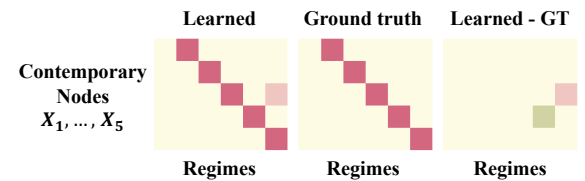


Figure 4: A showcase of the interventional targets results on synthetic data.

5.2.2 On real-world data center datasets. Table 3 presents the results on real data. It can be observed that our method not only achieves fewer C2A False but also learns a higher number of A2A True and C2C True relations. We can also find that introducing prior domain knowledge with LLM module can effectively understand the upstream and downstream relationship of variables in the system architecture, and avoid the influence of downstream variables on upstream variables, thus controlling the C2A False continues to be zero in the subsequent optimization. Besides, the standard deviation of each metric is relatively small as well. Therefore, RealTCD outperforms other approaches comprehensively in industrial scenarios by utilizing rich information from interventional data and prior domain knowledge.

Table 2: Results on synthetic datasets. \uparrow denotes the higher the better, and \downarrow denotes the lower the better. The best results are in bold in the setting of unknown interventional targets.

Targets	Causality	Method	5 nodes, 1 lag		10 nodes, 1 lag	
			SHD \downarrow	SID \downarrow	SHD \downarrow	SID \downarrow
Known	intra+inter	TECDI	1.55 \pm 2.30	1.82 \pm 2.40	3.91 \pm 5.05	10.64 \pm 10.35
		RealTCD	1.20 \pm 2.80	1.56 \pm 3.12	2.15 \pm 4.32	8.95 \pm 10.54
Unknown	intra+inter	DYNOTEARS	20.40 \pm 2.41	38.60 \pm 3.72	36.00 \pm 5.21	118.60 \pm 20.66
		PCMCI	18.10 \pm 4.43	24.10 \pm 3.11	62.00 \pm 17.15	118.30 \pm 24.08
		TECDI	11.90 \pm 4.75	17.70 \pm 8.49	27.40 \pm 10.69	60.80 \pm 25.74
		RealTCD	9.90 \pm 2.85	16.10 \pm 6.19	7.10 \pm 4.43	18.50 \pm 11.04
	intra	NeuralGC	14.90 \pm 2.28	20.00 \pm 0.00	31.30 \pm 4.72	85.50 \pm 6.36
		RealTCD	6.30 \pm 1.83	18.10 \pm 3.75	5.62 \pm 3.81	75.25 \pm 11.89

Table 3: Results on real-world datasets. \uparrow denotes the higher the better, and \downarrow denotes the lower the better. The best results are in bold in the setting of unknown interventional targets.

Targets	Causality	Method	All edges	C2A False \downarrow	A2C True \uparrow	A2A True \uparrow	C2C True \uparrow
Known	intra+inter	TECDI	85.6 \pm 12.46	4.00 \pm 6.85	5.80 \pm 3.16	0.70 \pm 1.34	2.80 \pm 1.32
		RealTCD	79.52 \pm 7.96	0.00 \pm 0.00	6.05 \pm 1.26	10.53 \pm 2.15	5.71 \pm 3.04
Unknown	intra+inter	DYNOTEARS	38.00 \pm 0.00	0.00 \pm 0.00	0.00 \pm 0.00	0.00 \pm 0.00	0.00 \pm 0.00
		PCMCI	181.60 \pm 32.26	32.90 \pm 5.00	13.20 \pm 2.86	7.50 \pm 5.87	5.00 \pm 2.49
		TECDI	57.60 \pm 10.67	2.40 \pm 1.51	1.50 \pm 1.84	1.80 \pm 1.48	0.40 \pm 0.97
		RealTCD	51.70 \pm 7.96	0.00 \pm 0.00	1.50 \pm 0.97	14.00 \pm 1.63	8.40 \pm 1.90
	intra	NeuralGC	104.10 \pm 41.09	25.70 \pm 19.47	1.90 \pm 4.01	5.20 \pm 3.71	4.00 \pm 3.65
		RealTCD	51.70 \pm 7.96	0.00 \pm 0.00	1.50 \pm 0.97	14.00 \pm 1.63	8.40 \pm 1.90

RealTCD in the "Unknown" targets setting, especially designed in our paper, achieves the best performance across all settings, even outperforming the "Known" targets setting. This is because the interventional targets provided by users are often not ground truth (people can only detect anomalous variables, but cannot confirm whether they are the ground truth interventional targets), which could potentially mislead the learning of algorithm. This further underscores the importance of using our method based on interventional data with unknown targets to deal with real-world cases.

5.3 Deeper Analysis

5.3.1 Ablation studies. In this section, we conduct ablation studies to verify the effectiveness of the proposed two modules in **RealTCD**, and the results are shown in Table 4.

We compare the ablated version 'RealTCD-intervention' that **removes the interventional module** in score-based temporal causal discovery and uses purely observational data in the same sample size. We observe that RealTCD-intervention tends to output significantly more edges making the comparisons unfair, so we calculate the ratio of the labeled edges learned to the total number of edges learned for further evaluation. We find that removing the interventional module significantly decreases the performance, especially for the metric ratio of A2A True and C2C True, which verifies the effectiveness of the proposed score-based temporal causal discovery method from interventional data.

Similarly, we compare the ablated version 'RealTCD-LLM' that **removes the LLM-guided meta initialization mechanism**. The

performance on real-world datasets significantly declines when the module is omitted, even to zero in terms of the A2A True metric, indicating that the module LLM-guided meta initialization mechanism can utilize prior information inside the abundant system textual information, and has distinct boosting effects on temporal causal discovery in real-world scenarios. This module's integration is pivotal because it primes the causal discovery process with a well-informed starting point, thereby reducing potential biases and improving the precision of causal inference.

5.3.2 Different LLM models. We also provide a variety of attempts on different LLMs and prompts with the real-world datasets [17, 57], where the first one choosing GPT-4 and prompt with implication and Chain-of-Thoughts (CoT) [45] is the one we used in our above experiments, and all results are shown in Table 5. Overall, GPT-4 is able to achieve better and more stable results.

6 DISCUSSION

6.1 Motivation and strengths of using LLMs

In real-world industrial systems, operations are often accompanied by extensive textual documentation such as logs, manuals, and system descriptions. These texts provide a rich source of untapped knowledge that directly relates to system behavior and operational dependencies. LLMs excel in mining such textual data for relevant information that informs causal analysis, thereby establishing an inherent connection between textual data and system operations.

Table 4: Ablation studies of the RealTCD modules on real-world datasets. \uparrow denotes the higher the better, and \downarrow denotes the lower the better. The best results in terms of metric ratios are in bold.

Method	All edges	C2A False \downarrow	A2C True \uparrow	A2A True \uparrow	C2C True \uparrow
RealTCD	51.70 \pm 7.96	0.00 \pm 0.00	1.50 \pm 0.97	14.00 \pm 1.63	8.40 \pm 1.90
Ratio of metrics / All edges	(%)	0.00 \pm 0.00	3.08 \pm 2.43	27.34 \pm 2.69	16.47 \pm 3.59
RealTCD-intervention	304.30 \pm 18.66	0.00 \pm 0.00	43.30 \pm 7.33	16.50 \pm 1.58	14.80 \pm 1.14
Ratio of metrics / All edges	(%)	0.00 \pm 0.00	14.17 \pm 1.75	5.43 \pm 0.54	4.87 \pm 0.36
RealTCD-LLM	38.80 \pm 1.87	0.00 \pm 0.00	0.10 \pm 0.32	0.00 \pm 0.00	0.40 \pm 0.70
Ratio of metrics / All edges	(%)	0.00 \pm 0.00	0.23 \pm 0.72	0.00 \pm 0.00	0.97 \pm 1.65

Table 5: Performance comparisons of different LLMs and prompt techniques in RealTCD on real-world datasets. \uparrow denotes the higher the better, and \downarrow denotes the lower the better.

Prompt No.	implication	CoT	Models	C2A False \downarrow	A2C True \uparrow	A2A True \uparrow	C2C True \uparrow
0	\checkmark	\checkmark	GPT-4	0	60	36	36
			GPT-3.5-turbo-instructor	0	8	0	0
1		\checkmark	GPT-4	0	68	0	0
			GPT-3.5-turbo-instructor	0	8	18	0
2			GPT-4	0	18	0	12
			GPT-3.5-turbo-instructor	0	32	0	0

In the "LLM-guided Meta Initialization" module, we utilize LLMs to incorporate domain knowledge and system structure information presented in textual form. This approach enables us to preliminarily extract potential causal relationships as a foundation for the discovery process. We outline **the irreplaceable strengths of using LLMs** over traditional deep learning approaches as follows:

- **Handling Textual Information:** While traditional causal discovery methods often overlook the rich textual data available in real-world systems, LLMs excel in processing and utilizing this data. This capability significantly enhances the accuracy and relevance of causal discovery outcomes. Although conventional language models can also process text, they lack the advanced capabilities of LLMs, as detailed in the next point.
- **Integration of Domain Knowledge:** Our method leverages LLMs not only to assimilate user inputs (e.g. the structure of a particular system) but also to integrate the vast domain-specific knowledge embedded within the LLMs (e.g. the operation law of a system), which may cover areas unfamiliar to the users. LLMs have access to extensive data within the same domain, often possessing more domain knowledge than the users. This integration is crucial for understanding complex systems where specific domain insights are vital for accurate causal inference.
- **LLM-guided Meta-Initialization:** As demonstrated in Section 5.3.1, this innovative module significantly enhances the quality of causal discovery compared to methods that do not use textual information. Traditional temporal causal discovery methods typically initialize by assuming all relationships may have causal links, then eliminate the non-existent ones, which can lead to suboptimal local solutions and high variance in results. By utilizing meta-knowledge extracted by LLMs to narrow the scope of causal discovery initially, we can significantly improve the stability and quality of the causal discovery algorithm.

The suitability of LLMs for enhancing causal discovery is also supported by a body of literature that demonstrates their effectiveness in extracting and applying domain knowledge in complex inference tasks [4, 9, 22, 41].

6.2 Limitation

We acknowledge that there are limitations related to the quality and completeness of the textual data in real-world applications [47]. Issues such as noise in the data, incomplete or missing text, and small sample sizes can potentially affect the performance of our method. These challenges are indeed inevitable and deserve further investigation.

6.3 Practical Implications

Though we emphasize the application of temporal causal discovery within AIOps, it is also helpful in various fields such as finance [20], healthcare [13], and social sciences [14] by uncovering the dynamic interrelations between variables over time. We discuss the **broad practical implications** of our method elaborately in Appendix C.

7 CONCLUSION

In this paper, we propose the **RealTCD** framework, a novel approach for temporal causal discovery in AIOps that circumvents the need for interventional targets and efficiently utilizes system textual information. Our method, with the proposed score-based temporal causal discovery and LLM-guided meta-initialization, has demonstrated its superiority over the existing baselines in both simulated and real-world datasets in terms of temporal causal discovery. The findings from **RealTCD** not only highlight its potential in enhancing causal analysis in complex IT systems but also open avenues for further research in AI-driven operations and maintenance in practical industrial scenarios.

ACKNOWLEDGMENTS

This work was supported in part by the National Key Research and Development Program of China No. 2020AAA0106300, National Natural Science Foundation of China (No. 62222209, 62250008, 62102222), Beijing National Research Center for Information Science and Technology Grant No. BNR2023RC01003, BNR2023TD03006, Alibaba Innovative Research Program and Beijing Key Lab of Networked Multimedia.

REFERENCES

- [1] Raghavendra Addanki, Shiva Kasiviswanathan, Andrew McGregor, and Cameron Musco. 2020. Efficient intervention design for causal discovery with latents. In *International Conference on Machine Learning*. PMLR, 63–73.
- [2] Vijay Arya, Karthikeyan Shanmugam, Pooja Aggarwal, Qing Wang, Prateeti Mohapatra, and Seema Nagar. 2021. Evaluation of causal inference techniques for AIOps. In *Proceedings of the 3rd ACM India Joint International Conference on Data Science & Management of Data (8th ACM IKDD CODS & 26th COMAD)*, 188–192.
- [3] Taiyu Ban, Lyuzhou Chen, Derui Lyu, Xiangyu Wang, and Huanhuan Chen. 2023. Causal Structure Learning Supervised by Large Language Model. *arXiv preprint arXiv:2311.11689* (2023).
- [4] Taiyu Ban, Lyuzhou Chen, Xiangyu Wang, and Huanhuan Chen. 2023. From query tools to causal architects: Harnessing large language models for advanced causal discovery from data. *arXiv preprint arXiv:2306.16902* (2023).
- [5] Amrita Bhattacharjee, Raha Moraffah, Joshua Garland, and Huan Liu. 2023. Towards LLM-guided Causal Explainability for Black-box Text Classifiers. <https://api.semanticscholar.org/CorpusID:262459118>
- [6] Philippe Brouillard, Sébastien Lachapelle, Alexandre Lacoste, Simon Lacoste-Julien, and Alexandre Drouin. 2020. Differentiable causal discovery from interventional data. *Advances in Neural Information Processing Systems* 33 (2020), 21865–21877.
- [7] Alessandro Castellano, Riccardo Crupi, Fabio Mercurio, Mario Mezzanzanica, Daniele Poterti, and Daniele Regoli. 2024. Marrying LLMs with Domain Expert Validation for Causal Graph Generation. (2024).
- [8] Chunkit Chan, Jiayang Cheng, Weiqi Wang, Yuxin Jiang, Tianqing Fang, Xin Liu, and Yangqiu Song. 2023. Chatgpt evaluation on sentence level relations: A focus on temporal, causal, and discourse relations. *arXiv preprint arXiv:2304.14827* (2023).
- [9] Lyuzhou Chen, Taiyu Ban, Xiangyu Wang, Derui Lyu, and Huanhuan Chen. 2023. Mitigating Prior Errors in Causal Structure Learning: Towards LLM driven Prior Knowledge. *arXiv preprint arXiv:2306.07032* (2023).
- [10] Kai-Hendrik Cohrs, Emiliano Diaz, Vasileios Sitokostantinou, Gherardo Varando, and Gustau Camps-Valls. 2023. Large Language Models for Constrained-Based Causal Discovery. In *AAAI 2024 Workshop on "Are Large Language Models Simply Causal Parrots?"*.
- [11] Frederick Eberhardt. 2012. Almost Optimal Intervention Sets for Causal Discovery. *arXiv:1206.3250* [cs.AI]
- [12] Tian Gao, Debarun Bhattacharjya, Elliot Nelson, Miao Liu, and Yue Yu. 2022. IDYNO: Learning Nonparametric DAGs from Interventional Dynamic Data. In *International Conference on Machine Learning*. PMLR, 6988–7001.
- [13] Chang Gong, Di Yao, Chuzhe Zhang, Wenbin Li, Jingping Bi, Lun Du, and Jin Wang. 2023. Causal discovery from temporal data. In *Proceedings of the 29th ACM SIGKDD Conference on Knowledge Discovery and Data Mining*, 5803–5804.
- [14] Anna Grzymala-Busse. 2011. Time will tell? Temporality and the analysis of causal mechanisms and processes. *Comparative Political Studies* 44, 9 (2011), 1267–1297.
- [15] George Gui and Olivier Toubia. 2023. The Challenge of Using LLMs to Simulate Human Behavior: A Causal Inference Perspective. *ArXiv abs/2312.15524* (2023). <https://api.semanticscholar.org/CorpusID:266133974>
- [16] Amin Jaber, Murat Kocoglu, Karthikeyan Shanmugam, and Elias Bareinboim. 2020. Causal discovery from soft interventions with unknown targets: Characterization and learning. *Advances in neural information processing systems* 33 (2020), 9551–9561.
- [17] Zhijing Jin, Yuen Chen, Felix Leeb, Luigi Gresle, Ojasv Kamal, Zhiheng Lyu, Kevin Blin, Fernando Gonzalez Aduato, Max Kleiman-Weiner, Mrinmaya Sachan, et al. 2024. Cladder: A benchmark to assess causal reasoning capabilities of language models. *Advances in Neural Information Processing Systems* 36 (2024).
- [18] Thomas Jiralerspong, Xiaoyin Chen, Yash More, Vedant Shah, and Yoshua Bengio. 2024. Efficient causal graph discovery using large language models. *arXiv preprint arXiv:2402.01207* (2024).
- [19] Diviyaa Kalainathan, Olivier Goudet, Isabelle Guyon, David Lopez-Paz, and Michèle Sebag. 2022. Structural agnostic modeling: Adversarial learning of causal graphs. *The Journal of Machine Learning Research* 23, 1 (2022), 9831–9892.
- [20] Prabhajan Kambadur, Aurélie C Lozano, and Ronny Luss. 2016. Temporal causal modeling. *Financial Signal Processing and Machine Learning* (2016), 41–66.
- [21] Tejas Kasetty, Divyat Mahajan, Gintare Karolina Dziugaite, Alexandre Drouin, and Dhanya Sridhar. 2024. Evaluating Interventional Reasoning Capabilities of Large Language Models. <https://api.semanticscholar.org/CorpusID:269004745>
- [22] Emre Kiciman, Robert Ness, Amit Sharma, and Chenhao Tan. 2023. Causal reasoning and large language models: Opening a new frontier for causality. *arXiv preprint arXiv:2305.00050* (2023).
- [23] Peiwen Li, Yuan Meng, Xin Wang, Fang Shen, Yue Li, Jialong Wang, and Wenwu Zhu. 2023. Causal Discovery in Temporal Domain from Interventional Data. In *Proceedings of the 32nd ACM International Conference on Information and Knowledge Management*, 4074–4078.
- [24] Xiaoyu Liu, Paiheng Xu, Junda Wu, Jiaxin Yuan, Yifan Yang, Yuhang Zhou, Fuxiao Liu, Tianrui Guan, Haoliang Wang, Tong Yu, et al. 2024. Large language models and causal inference in collaboration: A comprehensive survey. *arXiv preprint arXiv:2403.09606* (2024).
- [25] Stephanie Long, Tibor Schuster, Alexandre Piché, ServiceNow Research, et al. 2023. Can large language models build causal graphs? *arXiv preprint arXiv:2303.05279* (2023).
- [26] Qing Lyu, Shreya Havaldar, Adam Stein, Li Zhang, Delip Rao, Eric Wong, Marianna Apidianaki, and Chris Callison-Burch. 2023. Faithful chain-of-thought reasoning. *arXiv preprint arXiv:2301.13379* (2023).
- [27] Søren Wengel Mogensen, Karin Rathsmann, and Per Nilsson. 2023. Causal discovery in a complex industrial system: A time series benchmark. *arXiv preprint arXiv:2310.18654* (2023).
- [28] Narmada Naik, Ayush Khandelwal, Mohit Joshi, Madhusudan Atre, Hollis Wright, Kavya Kannan, Scott Hill, Giridhar Mamidipudi, Ganapati Srinivasa, Carlo Bifulco, et al. 2023. Applying Large Language Models for Causal Structure Learning in Non Small Cell Lung Cancer. *arXiv preprint arXiv:2311.07191* (2023).
- [29] Ignavier Ng, Shengyu Zhu, Zhuangyan Fang, Haoyang Li, Zhitang Chen, and Jun Wang. 2022. Masked gradient-based causal structure learning. In *Proceedings of the 2022 SIAM International Conference on Data Mining (SDM)*, SIAM, 424–432.
- [30] Roxana Pamfil, Nisara Sriwattanaworachai, Shaan Desai, Philip Pilgerstorfer, Konstantinos Georgatzis, Paul Beaumont, and Bryon Aragam. 2020. Dynotears: Structure learning from time-series data. In *International Conference on Artificial Intelligence and Statistics*. PMLR, 1595–1605.
- [31] Nick Pawlowski, James Vaughan, Joel Jennings, and Cheng Zhang. 2023. Answering causal questions with augmented llms. (2023).
- [32] Judea Pearl. 2009. *Causality*. Cambridge university press.
- [33] Jonas Peters and Peter Bühlmann. 2015. Structural intervention distance for evaluating causal graphs. *Neural computation* 27, 3 (2015), 771–799.
- [34] Juan F Rubio-Ramirez, Daniel F Waggoner, and Tao Zha. 2010. Structural vector autoregressions: Theory of identification and algorithms for inference. *The Review of Economic Studies* 77, 2 (2010), 665–696.
- [35] Jakob Runge. 2020. Discovering contemporaneous and lagged causal relations in autocorrelated nonlinear time series datasets. In *Conference on Uncertainty in Artificial Intelligence*. PMLR, 1388–1397.
- [36] Masayuki Takayama, Tadahisa Okuda, Thong Pham, Tatsuyoshi Ikenoue, Shingo Fukuma, Shohei Shimizu, and Akiyoshi Sannai. 2024. Integrating Large Language Models in Causal Discovery: A Statistical Causal Approach. *arXiv preprint arXiv:2402.01454* (2024).
- [37] Alex Tank, Ian Covert, Nicholas Foti, Ali Shojaie, and Emily B Fox. 2021. Neural granger causality. *IEEE Transactions on Pattern Analysis and Machine Intelligence* 44, 8 (2021), 4267–4279.
- [38] Jin Tian and Judea Pearl. 2013. Causal discovery from changes. *arXiv preprint arXiv:1301.2312* (2013).
- [39] Song Tong, Kai Mao, Zhen Huang, Yukun Zhao, and Kaiping Peng. 2024. Automating Psychological Hypothesis Generation with AI: Large Language Models Meet Causal Graph. *arXiv preprint arXiv:2402.14424* (2024).
- [40] Aniket Vashishtha, Abbavaram Gowtham Reddy, Abhinav Kumar, Saketh Bachu, Vineeth N Balasubramanian, and Amit Sharma. 2023. Causal Inference Using LLM-Guided Discovery. *ArXiv abs/2310.15117* (2023). <https://api.semanticscholar.org/CorpusID:264591509>
- [41] Aniket Vashishtha, Abbavaram Gowtham Reddy, Abhinav Kumar, Saketh Bachu, Vineeth N Balasubramanian, and Amit Sharma. 2023. Causal inference using llm-guided discovery. *arXiv preprint arXiv:2310.15117* (2023).
- [42] Dongjie Wang, Zhengzhang Chen, Yanjie Fu, Yanchi Liu, and Haifeng Chen. 2023. Incremental Causal Graph Learning for Online Root Cause Analysis. In *Proceedings of the 29th ACM SIGKDD Conference on Knowledge Discovery and Data Mining*, 2269–2278.
- [43] Xiao Wang, Peng Cui, Jing Wang, Jian Pei, Wenwu Zhu, and Shiqiang Yang. 2017. Community preserving network embedding. In *Proceedings of the AAAI conference on artificial intelligence*, Vol. 31.
- [44] Xiao Wang, Houye Ji, Chuan Shi, Bai Wang, Yanfang Ye, Peng Cui, and Philip S Yu. 2019. Heterogeneous graph attention network. In *The world wide web conference*, 2022–2032.
- [45] Jason Wei, Xuezhi Wang, Dale Schuurmans, Maarten Bosma, Fei Xia, Ed Chi, Quoc V Le, Denny Zhou, et al. 2022. Chain-of-thought prompting elicits reasoning in large language models. *Advances in Neural Information Processing Systems* 35 (2022), 24824–24837.

- [46] Moritz Willig, Matej Zečević, Devendra Singh Dhami, and Kristian Kersting. 2022. Probing for correlations of causal facts: Large language models and causality. (2022).
- [47] Moritz Willig, Matej Zečević, Devendra Singh Dhami, and Kristian Kersting. 2023. Causal parrots: Large language models may talk causality but are not causal. *preprint* 8 (2023).
- [48] Wenzhuo Yang, Kun Zhang, and Steven Hoi. 2022. A Causal Approach to Detecting Multivariate Time-series Anomalies and Root Causes. (2022).
- [49] Wenzhuo Yang, Kun Zhang, and Steven CH Hoi. 2022. Causality-based multivariate time series anomaly detection. *arXiv preprint arXiv:2206.15033* (2022).
- [50] Cheng Zhang, Stefan Bauer, Paul Bennett, Jiangfeng Gao, Wenbo Gong, Agrin Hilmkil, Joel Jennings, Chao Ma, Tom Minka, Nick Pawlowski, and James Vaughan. 2023. Understanding Causality with Large Language Models: Feasibility and Opportunities. *arXiv:2304.05524* [cs.LG]
- [51] Zeyang Zhang, Xingwang Li, Fei Teng, Ning Lin, Xueling Zhu, Xin Wang, and Wenwu Zhu. 2023. Out-of-Distribution Generalized Dynamic Graph Neural Network for Human Albumin Prediction. In *IEEE International Conference on Medical Artificial Intelligence*.
- [52] Ziwei Zhang, Xin Wang, Zeyang Zhang, Peng Cui, and Wenwu Zhu. 2021. Revisiting Transformation Invariant Geometric Deep Learning: Are Initial Representations All You Need? *arXiv preprint arXiv:2112.12345* (2021).
- [53] Zeyang Zhang, Xin Wang, Ziwei Zhang, Haoyang Li, Yijian Qin, Simin Wu, and Wenwu Zhu. 2023. LLM4DyG: Can Large Language Models Solve Spatio-Temporal Problems on Dynamic Graphs? *arXiv preprint arXiv:2310.17110* (2023).
- [54] Zeyang Zhang, Xin Wang, Ziwei Zhang, Haoyang Li, and Wenwu Zhu. 2023. Out-of-Distribution Generalized Dynamic Graph Neural Network with Disentangled Intervention and Invariance Promotion. *arXiv preprint arXiv:2311.14255* (2023).
- [55] Zeyang Zhang, Xin Wang, Ziwei Zhang, Zhou Qin, Weigao Wen, Hui Xue, Haoyang Li, and Wenwu Zhu. 2023. Spectral Invariant Learning for Dynamic Graphs under Distribution Shifts. In *Advances in Neural Information Processing Systems*.
- [56] Xun Zheng, Bryon Aragam, Pradeep K Ravikumar, and Eric P Xing. 2018. Dags with no tears: Continuous optimization for structure learning. *Advances in neural information processing systems* 31 (2018).
- [57] Yu Zhou, Xingyu Wu, Beicheng Huang, Jibin Wu, Liang Feng, and Kay Chen Tan. 2024. CausalBench: A Comprehensive Benchmark for Causal Learning Capability of Large Language Models. *arXiv preprint arXiv:2404.06349* (2024).

A DETAILED DESCRIPTION OF DATASETS

A.1 Synthetic Datasets Generation

We generate synthetic temporal data in two distinct steps, meticulously designed to emulate realistic causal structures and dependencies:

A.1.1 Graph structure sampling.

- DAG Sampling: We first sample the structure of intra-slice and inter-slice Directed Acyclic Graphs (DAGs) following the *Erdős-Rényi* model, a common approach for generating random graphs. This model allows us to control the sparsity of the DAG by setting a probability for the existence of each edge.
- Parameter Sampling: For the weighted adjacency matrices, we sample the edge weights to establish the strength and direction of causal influences:

Intra-slice Matrix W : The weights of the edges within the same time slice are sampled uniformly from the sets $[-1.0, -0.25] \cup [0.25, 1.0]$, ensuring non-trivial causal effects by excluding values close to zero.

Inter-slice Matrices A_k : For edges across different time slices, the weights are sampled uniformly from $[-1.0\alpha, -0.25\alpha] \cup [0.25\alpha, 1.0\alpha]$, $\alpha = 1/\eta^k$, $\eta \geq 1$, $k = 1, \dots, p$. The parameter k corresponds to the lag $k = 1, \dots, p$, introducing a decay factor that decreases the influence of past events over time, reflecting real-world temporal dynamics.

A.1.2 Time series data generation.

- Data Synthesis: Utilizing the sampled weighted graph, we generate time series data consistent with the standard structural vector autoregressive (SVAR) model as described by Rubio-Ramirez et al. [34]. The model equation $Y_0 = Y_0W + Y_1A_1 + \dots + Y_pA_p + Z$ integrates both intra-slice and inter-slice dependencies, where Y_0 represents the current state variables, Y_1, \dots, Y_p represent past state variables up to lag p , and Z is a vector of random variables drawn from a normal distribution, representing the noise in the system.
- Interventional Data: After generating the baseline time series data, we sample interventional targets from the nodes in Y_0 . We then create perfect interventional scenarios by severing the dependencies of these targeted nodes from their respective parents. Specifically, we set W_{ij} and A_{kij} to zero, where x_j is the variable in interventional targets and $x_i \in \mathcal{X}_{\pi_j^G}$.

By following this structured approach, we aim to generate a robust dataset that closely mimics the complexities and causal relationships inherent in real-world temporal systems.

A.2 Real-world Data Center Datasets Generation

Our LLM-enhanced temporal causal discovery method, which leverages interventional data, is **applicable across a wide range of industrial scenarios where both normal and anomalous states of data are present**. Examples include anomaly monitoring in power systems, analysis of factors affecting temperature, and financial risk monitoring. To date, there are no other type of publicly available real-world temporal datasets with interventional data suitable for evaluating such methods; previous studies typically rely

on synthetic data. Consequently, we utilized the self-constructed dataset from a data center. However, we acknowledge the importance of diversifying our datasets and will seek to include more varied industrial data in future evaluations of our model.

A.2.1 Scenario description. In contemporary data centers, the stability of IT equipment operation is paramount. Sophisticated air conditioning systems play a critical role in maintaining the operational integrity of these facilities. They manage the heat generated by IT equipment, ensuring that the indoor temperature remains within safe operational limits. This thermal management is vital for preventing equipment malfunction or failure due to overheating.

The internal architecture of a standard data center room is methodically organized to optimize airflow and temperature control. As illustrated in Figure 2, data centers are typically structured with rows of equipment cabinets labeled A, B, C, D, and so forth. These rows are separated by physical barriers that help isolate adjacent cabinet rows, effectively preventing the intermingling of hot and cold air streams. This isolation is crucial for efficient cooling as it helps maintain the integrity of cooled air distribution.

Strategically positioned along the sides of the room, Computer Room Air Conditioners (CRACs) play a pivotal role. These CRAC units facilitate a closed-loop configuration that is essential for preserving a stable environmental condition within the data center. By recycling the air within the room, CRACs ensure that the hot air exhausted from the server cabinets is cooled down and re-circulated.

Furthermore, the cooling architecture involves the use of chilled water systems, where cold air is not merely recycled but is generated through heat exchange with chilled water. The above system includes important components: *Chilled Water Inlet*, which is used for heat exchange with the air; *Water Valve Opening*, which controls the flow of chilled water; *Return Air Temperature*, which measures the air temperature after it has absorbed heat from the IT equipment, indicating the efficiency of heat removal.

Temperature sensors strategically deployed within the cold aisles collect real-time data. This continuous monitoring allows for the dynamic adjustment of air conditioning settings to respond promptly to any fluctuations in temperature. Specifically, by controlling the temperature and flow of chilled water, the CRACs adjust the supply air temperature directed into the cold aisles.

This comprehensive and sophisticated thermal management system ensures that data centers can operate continuously without interruption, providing the necessary cooling to maintain IT equipment in optimal working conditions. This setup not only protects valuable IT assets but also enhances energy efficiency and reduces the risk of downtime caused by equipment overheating.

A.2.2 Data acquisition. The dataset used in this study was sourced from a specific data center at Alibaba. It primarily focuses on the subsystem illustrated in the upper half of Figure 2, capturing the relationships between **air conditioning supply temperatures** and **cold aisle temperatures**. Specifically, it includes monitoring data from the cooling system of a particular room, covering the period from January 1st, 2023, to May 1st, 2023. In total, the dataset comprises 38 variables, which consist of 18 cold aisle temperatures from sensors located in the cold aisles and 20 air conditioning supply temperatures from Computer Room Air Conditioners (CRACs).

Due to strict alarm controls in the data center, overall alarms are quite rare. Even though some sensors exhibit fluctuations, these are typically controlled and do not trigger alarms. Hence, the data provided does not represent real alarm data but rather "anomalies" in the supply air temperatures and cold aisle temperatures. Anomaly points were identified by learning the normal distribution range from historical data, using the $n\text{-}\sigma$ method. Any data points that fell outside the $n\text{-}\sigma$ range (e.g., 3 to 5 times the standard deviation) of their respective variables were extracted as anomaly time points.

To collect this data, we acquired several time series of these 38 variables during both normal and abnormal states. During the abnormal conditions, data was sampled within 20 minutes of the detection of an anomaly, with each sampling interval set at 10 seconds.

A.2.3 Detailed data acquisition method.

- **Data Collection Scope:** The dataset encapsulates temperature readings from both the air conditioning supply (CRACs) and the cold aisles in a specific room of an Alibaba data center.
- **Time Frame:** Data was continuously monitored and recorded from January 1st, 2023, to May 1st, 2023.
- **Variable Details:** The dataset includes 38 distinct temperature variables, with 18 sourced from sensors in the cold aisles and 20 from the air conditioning supply units.
- **Anomaly Detection:** To identify anomalies in temperature readings, historical data was analyzed to establish a normal distribution range for each variable. Using the $n\text{-}\sigma$ method, any readings that deviated significantly (3 to 5 times the standard deviation) from this norm were flagged as anomalies.
- **Data Sampling for Anomalies:** For anomalies identified, additional data was collected at a high resolution. Data points were sampled every 10 seconds within a 20-minute window surrounding each identified anomaly, ensuring a detailed capture of conditions during abnormal states.

This approach allows for a comprehensive analysis of the cooling system's performance and the detection of any deviations from expected operational conditions. By modeling the anomalies into interventional data and further understanding these anomalies, the data center can optimize its cooling strategy and improve the overall stability of the IT equipment environment.

B EXAMPLE PROMPT

We provide a specific example of the prompt used for the data center dataset in our experiments, shown in Table 6.

C PRACTICAL IMPLICATIONS

In our paper, we emphasize the application of temporal causal discovery within AIOps to enhance IT systems' monitoring, troubleshooting, and predictive capabilities. This approach is crucial for improving system monitoring, anomaly detection[1], root cause analysis [42], failure prediction, and overall system optimization by elucidating the dynamic interactions between different system components and events over time.

Table 6: Prompts example for data center datasets.

Prompt D	<p>Role: You are an exceptional temporal causal discovery analyzer, with in-depth domain knowledge in the intelligent operation and maintenance of data center air-conditioning systems.</p> <p>Introduction: A directed temporal causal relationship between variables x_u and x_v can be represented as a tuple (x_u, x_v, t), signifying that the variable x_u, lagging t time units, causally influences the current state of variable x_v. The tuple $(x_u, x_v, 0)$ denotes contemporaneous causality if $t=0$; if $t>0$, the tuple (x_u, x_v, t) indicates time-lagged causality. Note that x_u and x_v must be different variables, as self-causality is not considered. Also, $(x_u, x_v, 0)$ and (x_u, x_v, t) for $t>0$ have the possibility to coexist, suggesting that contemporaneous and time-lagged causality between two variables might simultaneously occur sometimes.</p> <p>Our task is to unearth temporal causal relationships among variables, grounded on the subsequent information.</p>
Prompt I	<p>Domain knowledge: In modern data centers, maintaining stable IT equipment operation is critical. Advanced air conditioning systems manage the heat produced by equipment, sustaining a stable indoor climate. Equipment rows in a typical data center room are methodically arranged, with physical barriers separating adjacent rows to prevent air mixing. Computer room air conditioners (CRACs) flank the room, circulating cooling air and forming a closed loop for environmental stability. Multiple sensors in the cold aisle continuously monitor temperature, enabling prompt adjustments for stable IT equipment operation.</p> <p>There are 38 measuring points (20 CRACs and 18 sensors), represented by 'measuring_points_name:(x-axis_value, y-axis_value)' to indicate their relative positions. Using the bottom-left corner (CRAC_11) as the coordinate origin (0,0) and meters as the unit, the positions are as follows. There are 10 CRACs in the top row, from left to right: CRAC_1:(0,10.8), CRAC_2:(2.4,10.8), CRAC_3:(3.4,10.8), CRAC_4:(5.4,10.8), CRAC_5:(6.6,10.8), CRAC_6:(9,10.8), CRAC_7:(10.2,10.8), CRAC_8:(12.4,10.8), CRAC_9:(13.6,10.8), CRAC_10:(17,10.8); also 10 CRACs in the bottom row, from left to right: CRAC_11:(0,0), CRAC_12:(1.8,0), CRAC_13:(3.6,0), CRAC_14:(5.4,0), CRAC_15:(6.6,0), CRAC_16:(8.4,0), CRAC_17:(10.8,0), CRAC_18:(13.2,0), CRAC_19:(14.4,0), CRAC_20:(17,0). There are 5 columns of cabinets in the middle of the room, so there are 6 columns cold channels separated, each with three sensors, from the bottom right corner to the top left corner in turn: sensor_1:(17,3.9), sensor_2:(17,5.4), sensor_3:(17,7.5), sensor_4:(13.6,3.9), sensor_5:(13.6,5.4), sensor_6:(13.6,7.5), sensor_7:(10.2,3.9), sensor_8:(10.2,5.4), sensor_9:(10.2,7.5), sensor_10:(6.8,3.9), sensor_11:(6.8,5.4), sensor_12:(6.8,7.5), sensor_13:(3.4,3.9), sensor_14:(3.4,5.4), sensor_15:(3.4,7.5), sensor_16:(0,3.9), sensor_17:(0,5.4), sensor_18:(0,7.5). From the coordinates provided, you can know the relative position of the measuring points of the various devices in the computer room.</p> <p>Correspondingly, we consider 38 variables: air_1, ..., air_20 representing the supply temperatures of CRAC_1, ..., CRAC_20, and cold_1, ..., cold_18 denoting the temperatures in the cold aisle monitored by sensor_1, ..., sensor_18.</p>
Prompt C	<p>Task: Please identify all temporal causal relationships among the 38 variables (air_1 to air_20 and cold_1 to cold_18), considering only contemporaneous and 1 time-lagged causality ($t=0$ or 1). Conclude your response with the full answer as a Python list of tuples (x_u, x_v, t) after 'Answer:'. Write complete answers, don't cut them down.</p>
Prompt H	<p>CoT: Proceed methodically, step by step.</p>

Moreover, the utility of temporal causal discovery extends beyond IT operations into several other domains, thereby broadening our understanding and ability to manipulate complex systems across various fields:

- **Finance and Economics:** Temporal causal models can refine financial forecasting and investment strategies by revealing how economic variables influence each other over time, leading to more informed and effective decision-making [20].
- **Healthcare:** In medical research, understanding the temporal sequences of cause and effect can aid in predicting disease

progression, optimizing treatment plans, and improving patient outcomes [13, 28, 39, 51].

- **Social Sciences and Governance:** Temporal analysis is instrumental in political science and history for identifying causative factors behind regime changes and policy impacts, thus enhancing theoretical frameworks for understanding institutional transformations [14].

These examples illustrate the broad applicability and significant impact of temporal causal discovery in various sectors.